Borane Catalyzed Selective Diazo Cross-Coupling Towards Pyrazoles

Ayan Dasgupta,[a] Sanjukta Pahar,[a] Rasool Babaahmadi,[b] Lukas Gierlichs,[a] Brian F. Yates,[b] Alireza Ariafard,[b,*] and Rebecca L. Melen[a,*]

[a] Cardiff Catalysis Institute, School of Chemistry, Cardiff University
    Main Building, Park Place, Cardiff, CF10 3AT, Cymru/Wales, United Kingdom
    E-mail: MelenR@cardiff.ac.uk
[b] School of Natural Sciences (Chemistry), University of Tasmania, Private Bag 75, Hobart, Tasmania 7001, Australia
    E-mail: alireza.ariafard@utas.edu.au

Abstract: Decomposition of donor-acceptor diazo compounds leads to the formation of reactive carbene intermediates. These can undergo a wide variety of carbene transfer reactions to yield synthetically useful products. Herein, we report a selective borane catalyzed cyclization reaction from the combination of two different diazo compounds to afford N-substituted pyrazoles. The selective decomposition of the more reactive α-aryl α-diazoester and subsequent reaction with a vinyl diazoacetate produces N-alkylated pyrazoles in a regioselective manner. Catalytic amounts of tris(pentafluorophenyl)borane (10 mol%) were employed to afford the pyrazole products (36 examples) in yields from 59 to 80%. Extensive DFT studies have been undertaken to interpret the mechanism for this reaction which was found to go through two tandem catalytic cycles, both catalyzed by $B(C_6F_5)_3$.

Keywords: Diazoester; Pyrazole; Carbene; Tris(pentafluorophenyl)borane; Density Functional Theory

Introduction

Borane compounds have a low toxicity[1] and are commonly used in pharmaceutical synthesis.[2] They play a significant role in medicinal chemistry and the agrochemical industry. They are also an essential micronutrient for plants being found in several natural products.[3] The importance of boranes in the pharmaceutical industry, as well as the low toxicity of their hydrolysis products, renders their potential use as a catalyst in organic synthesis particularly attractive.[4] Boranes possess an empty *p*-orbital which can be accessed by a lone pair of electrons from a Lewis base leading to a Lewis acid-base adduct.[5] This reactivity has been exploited successfully for the activation of many organic substrates in synthetic transformations.[6] Although, the simple Lewis acid $BF_3 \cdot OEt_2$ has been used widely for these reactions,[7] fluorinated triaryl-

boranes $B(Ar^F)_3$ occasionally exhibit superior catalytic activity and improved (or alternate) selectivity due to the increased steric congestion around the boron center.[8] In early examples, Piers and Yamamoto disclosed the catalytic activities of $B(C_6F_5)_3$ in hydrosilylation,[9] and aldol-type/Michael addition reactions.[10] These ground-breaking results provoked interest in the use of halogenated triarylboranes as metal-free catalysts for a range of transformations.[11]

The divergent reactivities of donor-acceptor diazo compounds have led to their prominence as important scaffolds for the synthesis of a plethora of compounds.[12] Decomposition of donor-acceptor diazo compounds using metal catalysts to generate metal carbenoids has been extensively studied.[13] Conversely the generation of carbenes from diazo compounds catalyzed by boranes is a relatively new research interest.[14] Recent discoveries have disclosed both the

stoichiometric[15] and catalytic[16] reactions of halogenated triarylboranes with α-aryl α-diazoesters. In both cases, the activation of the α-aryl α-diazoester by the borane through O→B adduct formation is the crucial step in the generation of the carbene.

In the present study, we wanted to examine the $B(C_6F_5)_3$ (10 mol%) catalyzed reaction between vinyl diazoacetates and α-aryl α-diazoesters to afford C=C cross-coupled products which could be further utilized as a scaffold for stereoselective cyclization reactions.

However surprisingly, our initial experimental results revealed the selective decomposition of the donor-acceptor α-aryl α-diazoester compounds when reacted with vinyl diazoacetates, catalyzed by B-$(C_6F_5)_3$. The formation of one carbene intermediate and subsequent reaction with the vinyl diazoacetates afforded synthetically useful pyrazole moieties. The discriminatory decomposition of one diazoester over another is rather unusual. In 2015, Sun *et al.* demonstrated a ligand-controlled gold catalyzed reaction protocol for the selective decomposition of one diazoester over another.[17] However, metal-free synthesis of pyrazoles using diazoesters remains unexplored.

Nitrogen based heterocyclic compounds display a wide range of medicinal applications, therefore a metal-free synthesis towards these compounds is highly desirable.[18] Pyrazole derivatives have important applications in medicinal chemistry and have been successfully employed as anti-inflammatory, analgesic, antipyretic, antiviral, antibacterial, and anticancer agents.[19]

Relating to this study, several research groups have previously studied the selective decomposition of a mixture of two diazo compounds (e.g. a vinyl diazoacetate and a donor-acceptor α-aryl α-diazoester) using metal catalysts such as Rh,[20] Ru,[21] Ir,[22] Au,[23] and Cu.[24] In most cases, decomposition of both diazo compounds occurs to generate the respective metal carbenoid which can then either generate the C=C cross-coupled or homo-coupled product.

Results and Discussion

We began our investigations by studying the reaction of a vinyl diazoacetate[25] **1a** with a donor-acceptor α-aryl α-diazoester compound **2a** in the presence of catalytic amounts of $B(C_6F_5)_3$. Isolation of the products following the reaction showed that pyrazole formation was favored over the generation of the C=C homo- or hetero-coupled products. The product was formed as two different N-alkylated isomers **3** (major) and **3′** (minor) (Table 1).

Reaction optimization: Following the discovery that $B(C_6F_5)_3$ can catalyze pyrazole formation, we optimized the reaction conditions employing compounds **1a** and **2a** as model substrates to generate **3** in

Table 1. Optimization of the reaction conditions for the cyclization reactions of vinyl diazoacetate **1a** with α-aryl α-diazoester **2a**.
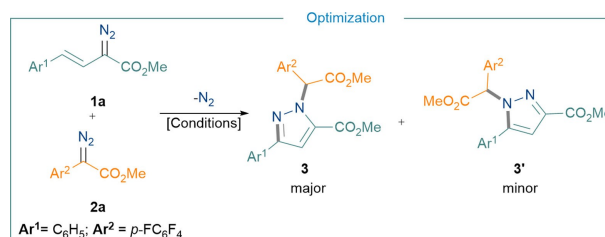
Entry	Lewis acid (10 mol%)	Solvent	Temp (°C)	3:3′[a]	Yield (%)[b]
1	–	CH_2Cl_2	rt	–	–
2	–	CH_2Cl_2	40	–	–
3	–	$C_2H_4Cl_2$	85	1:0.7	38
4	$BF_3 \cdot OEt_2$	CH_2Cl_2	40	–	–
5	*p*-TsOH	CH_2Cl_2	40	1:0.8	25
6	TfOH	CH_2Cl_2	40	1:0.8	31
7	2,4,6-BAr^F	CH_2Cl_2	40	1:0.7	42
8	3,4,5-BAr^F	CH_2Cl_2	40	1:0.8	33
9	$B(C_6F_5)_3$	CH_2Cl_2	40	1:0	63
10	$B(C_6F_5)_3$	toluene	40	1:0.8	44
11	$B(C_6F_5)_3$	toluene	85	1:0.8	40
12	$B(C_6F_5)_3$	Et_2O	40	–	–
13	$B(C_6F_5)_3$	MeCN	50	–	–
14	$B(C_6F_5)_3$	THF	50	–	–
15	$B(C_6F_5)_3$	$C_2H_4Cl_2$	60	1:0	80
16	$B(C_6F_5)_3$[b]	$C_2H_4Cl_2$	85	1:0.6	52
17	$B(C_6F_5)_3$[c]	$C_2H_4Cl_2$	60	1:0	42

Reaction conditions: all reactions were carried out on a 0.1 mmol scale;
[a] ratio between **3** and **3′** was determined from crude ¹H NMR spectra;
[b] yields reported are isolated yields of **3** only;
[c] 5 mol% $B(C_6F_5)_3$ was used.

high yields regio-selectively (Table 1). In the absence of a catalyst, no products (**3** or **3′**) formation were observed after 20–22 h in CH_2Cl_2 at room temperature or 40°C (Table 1, entries 1–2). Refluxing (85°C) the reaction mixture in 1,2-dichloroethane (1,2-$C_2H_4Cl_2$) afforded the cyclized N-substituted product **3** in poor yields of 38% (Table 1, entry 3). ¹H NMR spectral analysis of the crude reaction mixture indicates the formation of the two products in a 1:0.7 ratio of **3a**:**3a′**. Multinuclear NMR spectroscopic analysis and high-resolution mass spectrometric data of the respective pure compounds unambiguously confirmed the formation of the two regioisomeric products (**3a**, 38%; **3a′** 21%). Employing the commercially available, Lewis acidic borane $BF_3 \cdot OEt_2$ (Table 1, entry 4) as a catalyst (10 mol%) in CH_2Cl_2 at 40°C resulted in a complicated reaction mixture, with no expected product formation observed. Use of catalytic amounts of the Brønsted acids *p*-toluenesulfonic acid (*p*TsOH) and

trifluoromethane sulfonic acid (TfOH) showed poor regioselectivities (1:0.8) and afforded the desired product **3** in poor yields (25% and 31% respectively; Table 1, entries 5 and 6). Lewis acidic triarylfluoroboranes were also tested for this reaction; both B(2,4,6-$F_3C_6H_2)_3$/(2,4,6-BAr^F) and B(3,4,5-$F_3C_6H_2)_3$/(3,4,5-BAr^F) (Table 1, entries 7 and 8) again showed poor regioselectivities (1:0.7/0.8) but slightly improved yields of **3** (42% and 33% respectively). However, to our surprise, when catalytic amounts of B($C_6F_5)_3$ were employed in CH_2Cl_2 (Table 1, entry 9), excellent regioselectivity of **3a**:**3a′** was observed (1:0) albeit in moderate yields (63%). Various solvents were subsequently screened to improve the yield of the product. The reaction between **1a** and **2a** in toluene at 40°C and 85°C both afforded lower yields and showed poorer regioselectivities compared with CH_2Cl_2 (Table 1, entries 10 and 11). The use of coordinating solvents such as diethyl ether, acetonitrile, and tetrahydrofuran completely inhibited the reaction and no product formation was observed (Table 1, entries 12–14). The highest yield for **3a** (80%), was obtained using 1,2-$C_2H_4Cl_2$ as the solvent, with only a single regioisomeric product formed at 60°C (Table 1, entry 15). However, reaction at higher temperatures (85°C) led to the formation of a regioisomeric mixture (**3a**:**3a′** = 1:0.6) (Table 1, entry 16). Reducing the catalytic loading to 5 mol% lowered the yield of the product significantly (42%, Table 1, entry 17). Based on these screening results, it was decided to carry out all reactions in 1,2-$C_2H_4Cl_2$ with 10 mol% B($C_6F_5)_3$ loading, and the optimum temperature was set to 60°C.

Reaction scope: With these optimized reaction conditions in hand, a substrate scope was explored to examine the generality of the reported system (Scheme 1). Vinyl diazoacetates bearing electronically neutral (H, **1a**), electron withdrawing/π-releasing (*p*-F, **1b**; *p*-Cl, **1c**; *p*-Br, **1d**), and electron donating (*o*-Me, **1e**; *p*-OMe, **1f**) groups were employed for the reaction with various α-aryl α-diazoesters (*p*-F, **2a**; *p*-Cl, **2b**; *p*-H, **2c**; *p*-Me, **2d**). All substrate combinations afforded the N-alkylated pyrazole compounds (36 examples) regioselectively in good to excellent isolated yields of 59–80% (**3a**–**3x**).

Interestingly, when the α-aryl α-diazoester bearing an electron donating group (*p*-OMe, **2e**) is employed, the yield of **3** is slightly lower (59–66%) and the reaction is less selective with 10–14% of the regioisomer **3′** being formed (**3y**–**3ad**). In these cases, both isomers were isolated and characterized by multinuclear NMR spectroscopy and high-resolution mass spectrometry. All isomeric ratios (**3y**:**3y′**, **3z**:**3z′**, **3aa**:**3aa′**, **3ab**:**3ab′**, **3ac**:**3ac′**, and **3ad**:**3ad′**) were determined from ^{1}H NMR analysis of the crude reaction mixture. Limitations of the reaction included the aliphatic diazoester ethyl diazoacetate and the

electron deficient symmetrical diazoester dimethyl 2-diazomalonate which failed to react with vinyl diazoacetates to afford the pyrazole product. Formation of the N-alkylated pyrazole was also confirmed by X-ray diffraction analysis. Slow evaporation of saturated solutions of compound **3a**, **3i**, and **3k** in CH_2Cl_2 afforded crystals suitable for single crystal X-ray diffraction analysis (Figure 1 and ESI).

DFT Studies: After demonstrating a wide substrate scope, we turned our attention to understanding the mechanism of N-alkylated pyrazole synthesis as well as explaining the selectivity of the reaction. To investigate the reaction pathway, we undertook DFT calculations in CH_2Cl_2 at the SMD/M06-2X-D3/def2-TZVP//SMD/M06-2X/6-31G(d) level of theory.

The proposed reaction mechanism is shown in Scheme 2 based upon the DFT calculated free energy profile depicted in Figure 2. Extensive DFT calculations showed that the formation of N-alkylated pyrazoles can be explained by two concurrent catalytic cycles. In the first cycle, the Lewis acidic borane activates the α-aryl α-diazoester by coordinating to the carbonyl functionality generating **2a**·B($C_6F_5)_3$. Coordination of B($C_6F_5)_3$ with **2a** is found to be energetically favorable by 1.5 kcal/mol and reversible. Loss of
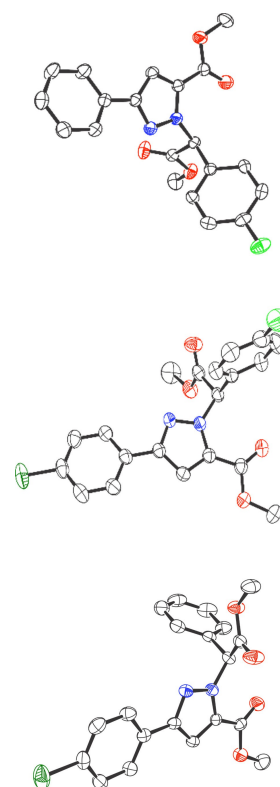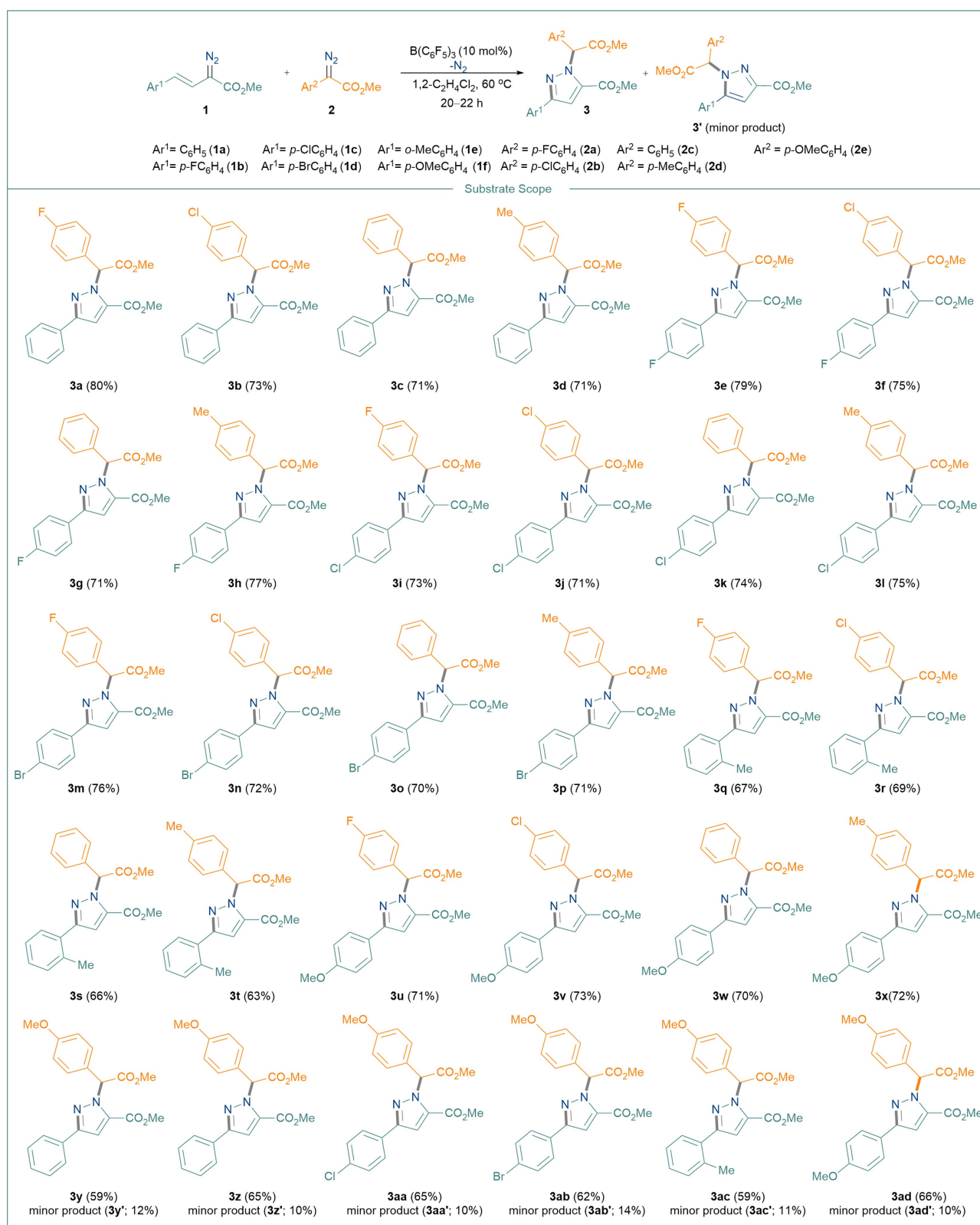

Figure 1. Solid-state structure of compound **3a** (top), **3i** (middle), and **3k** (bottom). Thermal ellipsoids drawn at 50% probability. Carbon: black; oxygen: red; fluorine: light green; chlorine: dark green; nitrogen: blue.

Scheme 1. Cascade cyclization reaction between vinyl diazoacetates (**1**) and α-aryl α-diazoesters (**2**). All the reactions were carried out on a 0.1 mmol scale. Yields reported are isolated yields.
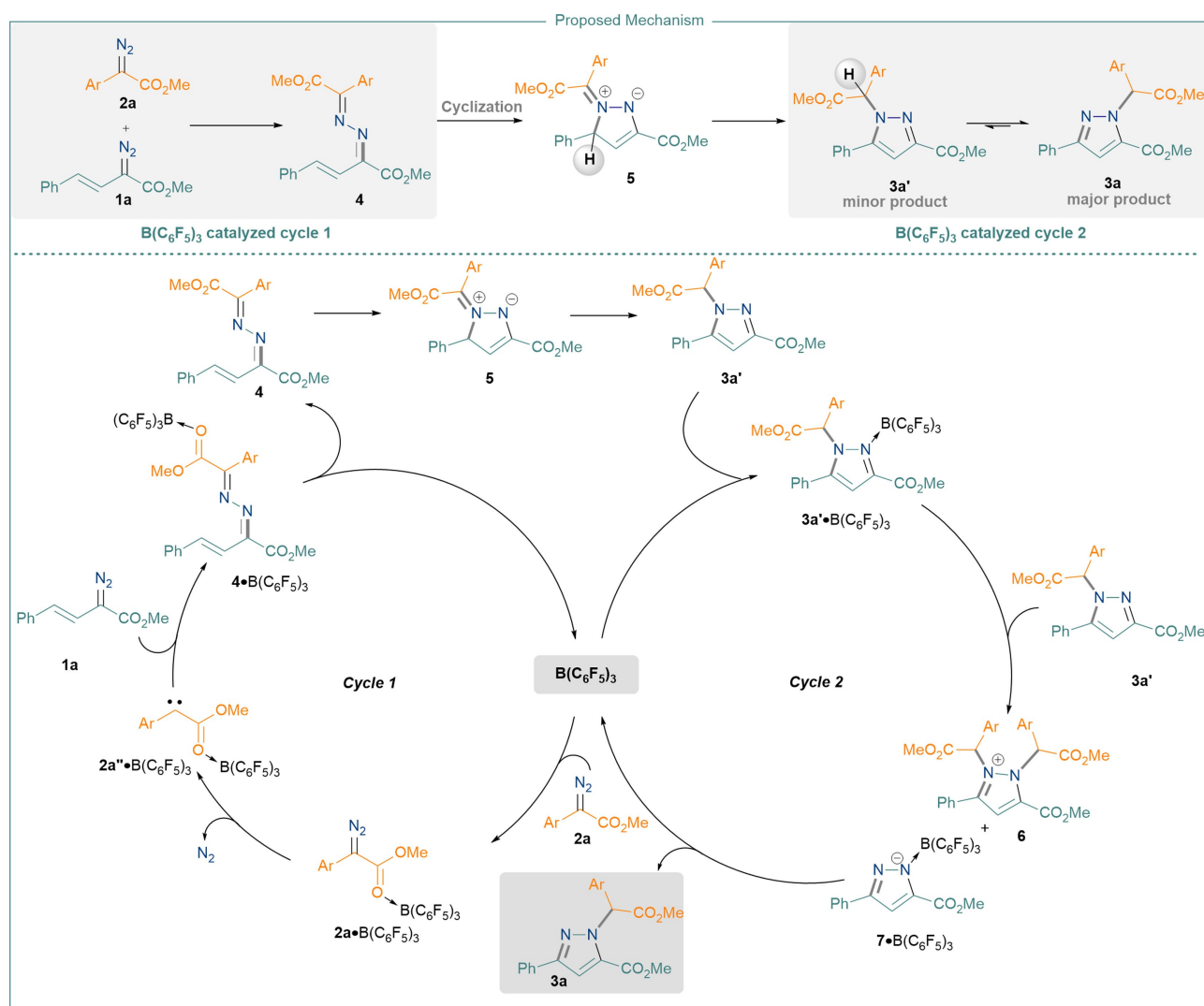
Scheme 2. Proposed reaction mechanism for pyrazole formation. Ar = *p*-FC$_6$H$_4$.

N_2 yields a reactive $B(C_6F_5)_3$ bound carbene **2 a"** that is immediately trapped by the second diazo compound (vinyl diazoacetate, **1 a**) to afford an energetically stable hydrazine as a borane adduct [**4·B(C_6F_5)_3**]. $B(C_6F_5)_3$ is then released to continue the catalytic *cycle 1*. In the next step, **4** undergoes an off cycle intramolecular cyclization to form heterocycle **5**. Proton transfer through a 1,3-hydrogen shift then leads to the formation of kinetically stable pyrazole isomer **3 a′** which is the minor product observed in a few selected examples e.g. when the *p*-OMe diazo compound **2 e** is employed. **3 a′** is then the starting point for *cycle 2* in which the minor isomer **3 a′** is converted to the more stable (0.7 kcal/mol) isomer **3 a** catalyzed by $B(C_6F_5)_3$. In *cycle 2*, **3 a′** forms an adduct with $B(C_6F_5)_3$ [**3 a′·B-(C_6F_5)_3**] which further reacts with another molecule of **3 a′** to afford the more thermodynamically stable isomer **3** *via* the formation of ions **6** and **7·B(C_6F_5)_3**.

The overall energy required for *cycle 2* was found to be 13.7 kcal/mol which is much lower than that for the uncatalyzed mechanism (46.4 kcal/mol) where the reaction proceeds through the formation of ions **6** and **7** (Figure 2, bottom). The energy difference between **3 a** (major product) and **3 a′** (minor product) is less than what we expected. This can be attributed to a minor error in the calculation and level of theory used. This claim is supported by our calculations at the SMD/B3LYP/def2-TZVP//SMD/M06-2X/6-31G(d) level of theory, which confirms that energy difference between **3 a** (major product) and **3 a′** (minor product) is larger with a value of 1.5 kcal/mol.

Furthermore, we carried out an experiment where compound **3 ad′** was reacted with 1.3 equiv. of **2 e** using 10 mol% $B(C_6F_5)_3$ in 1,2-$C_2H_4Cl_2$ at the optimum temperature 60 °C (Scheme 3). After 22 h, ^{1}H NMR analysis of the crude reaction mixture showed the formation of **3 ad** as the major product. ^{1}H NMR
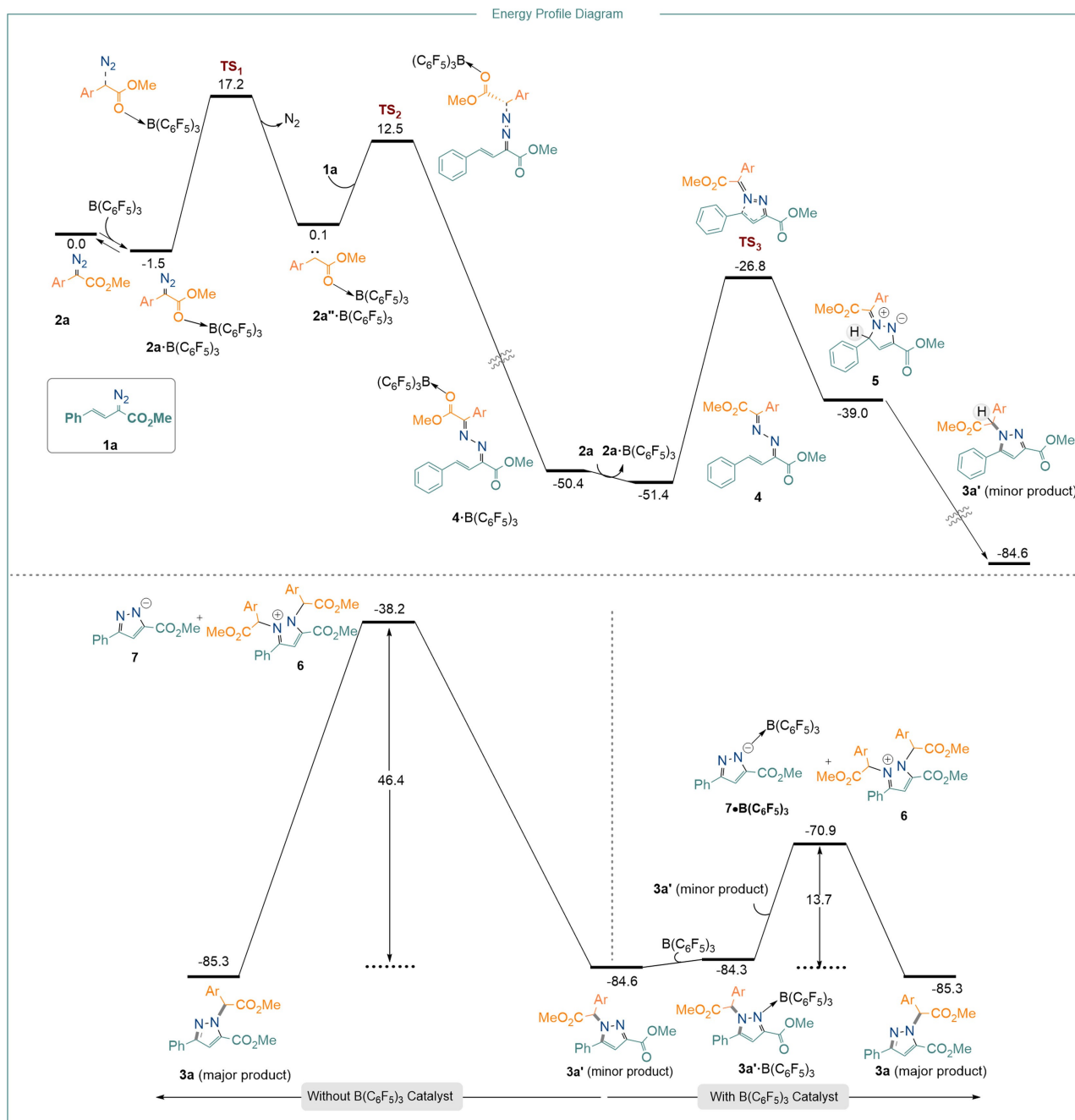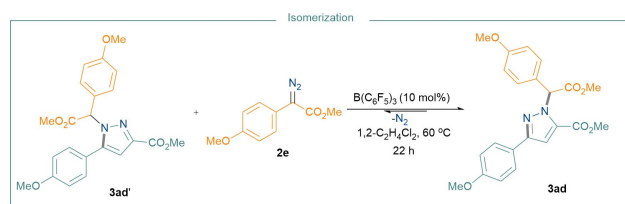
Figure 2. DFT computed reaction pathways for the formation of pyrazole-alkylated compound from the reaction of methyl (*E*)-2-diazo-4-phenylbut-3-enoate (**1 a**) and methyl 2-diazo-2-(4-fluorophenyl)acetate (**2 a**) in CH₂Cl₂ calculated using SMD/M06-2X-D3/def2-TZVP//SMD/M06-2X/6-31G(d) level of theory. The relative free energies are given in kcal/mol. Ar = *p*-FC₆H₄.

Scheme 3. Isomerization study. (0.1 mmol scale).

spectroscopy showed the presence of both **3 ad′** and **3 ad** in an approximate 4:1 ratio (see SI, Figure S108 and S109). Another potential mechanism for *cycle 1* is the initial formation of pyrazole **9** from **1 a** followed by N–H insertion of **2 a″**·B(C₆F₅)₃ to afford the **3 a′** (Scheme 4). *Cycle 2* then converts the **3 a′** to **3 a**. Indeed, if we independently synthesise **9** according to literature procedures[26] (See SI Figure S110 and S111) and subject this to the reaction conditions, then we
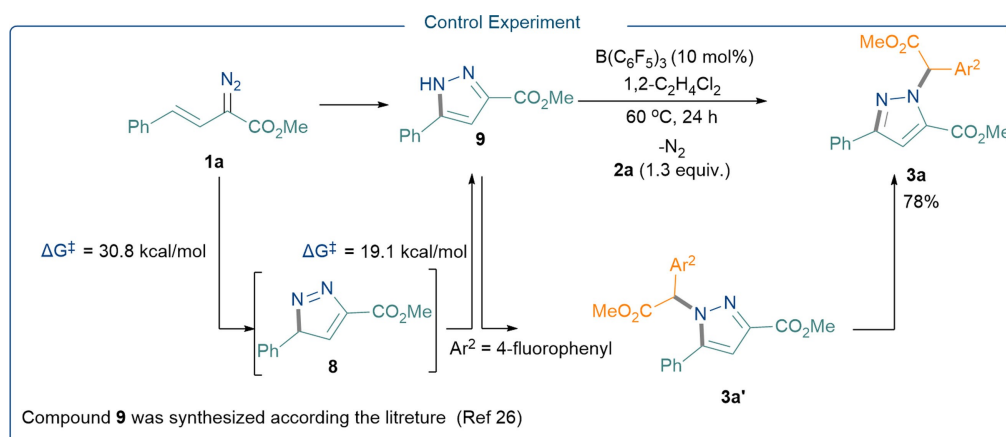
Scheme 4. Formation of **9** and control reaction between **9** and **2 a**.

observe the formation of **3 a** in 78% isolated yield. Moreover, formation of **3 a′** was also noticed and analysis of the crude ^{1}H NMR spectrum reveals that **3 a** and **3 a′** are formed in an approximate 1:0.08 ratio (See Figure S112 and 113). This clearly supports our proposed second catalytic cycle for conversion of **3 a′** to **3 a**. In order to determine which mechanism is operating for *cycle 1*, we turned to DFT studies (See SI Figure S117). In these studies, formation of **9** *via* **8** from **1 a** is energetically less favorable as the reaction proceed through the transition structure **TS$_{1a–8}$**, followed by a 1,2-proton shift to yield **9** with $\Delta G_{rxn} = -35.9$ kcal/mol. The overall activation barrier for this process is 30.8 kcal/mol (see SI Figure S117), corroborating the experimental result that such a reaction requires a high temperature to occur. This is higher in energy than the calculated pathway for *cycle 1*. Thus, while cyclization followed by N–H insertion is possible, our studies support the calculated pathway shown in Figure 2 which indicates that the borane catalyst accelerates the cyclization process.

Conclusion

In conclusion, a metal-free synthetic protocol has been developed to afford synthetically useful N-alkylated pyrazole products in a selective manner. Using 10 mol% catalytic loading of B(C$_6$F$_5$)$_3$, 36 examples of the pyrazole products were formed in yields from 59 to 80%. A detailed mechanistic study, using DFT analysis highlighted the possible reaction pathway for the formation of regioselective N-alkylated pyrazoles in which two B(C$_6$F$_5$)$_3$ catalyzed cycles work together. Firstly, to generate the pyrazole core, and secondly to isomerize the pyrazole into the major isomer observed in the reaction. The reported synthetic methodology for metal-free synthesis of pyrazoles will most likely draw the attention of both academic and industrial research for making biologically important molecules without

the need for toxic transition metal catalysts. The detailed DFT calculations will aid future exploitations of this reactivity and help direct catalyst design in the future.

Experimental Section

General procedure for the synthesis of pyrazoles. Tris(pentafluorophenyl)borane, B(C$_6$F$_5$)$_3$ (10 mol%) was dissolved in 1,2-C$_2$H$_4$Cl$_2$ (0.5 mL) and added to a 1,2-C$_2$H$_4$Cl$_2$ solution (0.5 mL) of the α-aryl α-diazoester (1.3 equiv.). The vinyl diazoacetate (1 equiv.) was dissolved separately in 1,2-C$_2$H$_4$Cl$_2$ (0.5 mL) and added dropwise to the reaction mixture. The reaction tube was sealed in the glove box under a nitrogen atmosphere and heated at 60 °C for 20–24 h. All volatiles were removed in vacuo and the crude reaction mixture purified via preparative thin layer chromatography using hexane/ethyl acetate as eluent.

Crystallographic data for compounds **3 a**, **3 i**, and **3 k** have been deposited in the Cambridge Crystallographic Data Centre under CCDC codes 2068708, 2068710, and 2068713. The data can be obtained free of charge from The Cambridge Crystallographic Data Centre via https://www.ccdc.cam.ac.uk/data request/cif/. Information about the data that underpins the results presented in this article, including how to access them, can be found in the Cardiff University data catalogue at http://doi.org/10.17035/d.2021.0148228396.

Advanced Synthesis & Catalysis

References

[1] F. H. Nielsen, *Plant Soil* **1997**, *193*, 199–208.

[2] For selected reviews see: a) S. J. Baker, J. W. Tomsho, S. J. Benkovic, *Chem. Soc. Rev.* **2011**, *40*, 4279–4285; b) J. Plesek, *Chem. Rev.* **1992**, *92*, 269–278; c) G. F. S. Fernandes, W. A. Denny, J. L. Dos Santos, *Eur. J. Med. Chem.* **2019**, *179*, 791–804.

[3] a) F. Yang, M. Zhu, J. Zhang, H. Zhou, *MedChemComm* **2018**, *9*, 201–211; b) Y. Chen, B. Shoichet, R. Bonnet, *J. Am. Chem. Soc.* **2005**, *127*, 5423–5434; c) R. Baggio, D. Elbaum, Z. F. Kanyo, P. J. Carroll, R. C. Cavalli, D. E. Ash, D. W. Christianson, *J. Am. Chem. Soc.* **1997**, *119*, 8107–8108; for a selected review on the use of boranes in agrochemistry see: d) F. Shireen, M. A. Nawaz, C. Chen, Q. Zhang, Z. Zheng, H. Sohail, J. Sun, H. Cao, Y. Huang, Z. Bie, *Int. J. Mol. Sci.* **2018**, *19*, 1856.

[4] a) E. A. Patrick, W. E. Piers, *Chem. Commun.* **2020**, *56*, 841–853; b) J. W. B. Fyfe, A. J. B. Watson, *Chem* **2017**, *3*, 31–55.

[5] a) C. Weetman, S. Inoue, *ChemCatChem* **2018**, *10*, 4213–4228; b) J. R. Lawson, R. L. Melen, in *Organometallic Chemistry Volume 41* **2017**, The Royal Society of Chemistry, pp. 1–27.

[6] a) J. R. Lawson, R. L. Melen, *Inorg. Chem.* **2017**, *56*, 8627–8643; b) G. Erker, *Dalton Trans.* **2005**, *2005*, 1883–1890.

[7] a) S. Muthusamy, M. Malarvizhi, E. Suresh, *Asian J. Org. Chem.* **2021**, *10*, 170–175; b) C. Xu, J. Xu, *Org. Biomol. Chem.* **2020**, *18*, 127–134; c) M. K. Ghorai, A. Kumar, D. P. Tiwari, *J. Org. Chem.* **2010**, *75*, 137–151; d) N. R. Mente, J. D. Neighbors, D. F. Wiemer, *J. Org. Chem.* **2008**, *73*, 7963–7970; e) Q. Zhang, S. Sun, J. Hu, Q. Liu, J. Tan, *J. Org. Chem.* **2007**, *72*, 139–143; f) G. W. Kabalka, N.-S. Li, D. Tejedor, R. R. Malladi, S. Trotman, *J. Org. Chem.* **1999**, *64*, 3157–3161.

[8] J. L. Carden, A. Dasgupta, R. L. Melen, *Chem. Soc. Rev.* **2020**, *49*, 1706–1725.

[9] D. J. Parks, W. E. Piers, *J. Am. Chem. Soc.* **1996**, *118*, 9440–9441.

[10] I. Kazuaki, H. Naoyuki, F. Miyuki, Y. M. Mayumi, Y. Hisashi Bull, *Chem. Soc. Jpn.* **1995**, *68*, 1721–1730.

[11] L. Marc-André, C. Marc-André, R. Étienne, F. Frédéric-Georges, *Science* **2015**, *349*, 513–516.

[12] For selected reviews see: a) D. Zhu, L. Chen, H. Fan, Q. Yao, S. Zhu, *Chem. Soc. Rev.* **2020**, *49*, 908–950; b) Q.-Q. Cheng, Y. Deng, M. Lankelma, M. P. Doyle, *Chem. Soc. Rev.* **2017**, *46*, 5425–5443; also see: c) N. R. O'Connor, P. Bolgar, B. M. Stoltz, *Tetrahedron Lett.* **2016**, *57*, 849–851; d) J. L. Brewbaker, H. J. Hart, *J. Am. Chem. Soc.* **1969**, *91*, 711–715; e) D. W. Adamson, J. Kenner, *J. Chem. Soc.* **1935**, *59*, 286–289.

[13] For selected reviews see: a) B. D. Bergstrom, L. A. Nickerson, J. T. Shaw, L. W. Souza, *Angew. Chem. Int. Ed.* **2021**, *60*, 6864–6878; b) H. M. L. Davies, J. R. Denton, *Chem. Soc. Rev.* **2009**, *38*, 3061–3071.

[14] a) K. S. Egorova, V. P. Ananikov, *Organometallics* **2017**, *36*, 4071–4090; b) Q.-L. Zhou, *Angew. Chem. Int. Ed.* **2016**, *55*, 5352–5353; *Angew. Chem.* **2016**, *128*, 5438–5439.

[15] a) M. Santi, D. M. C. Ould, J. Wenz, Y. Soltani, R. L. Melen, T. Wirth, *Angew. Chem. Int. Ed.* **2019**, *58*, 7861–7865; *Angew. Chem.* **2019**, *131*, 7943–7947; b) C. Tang, Q. Liang, A. R. Jupp, T. C. Johnstone, R. C. Neu, D. Song, S. Grimme, D. W. Stephan, *Angew. Chem. Int. Ed.* **2017**, *56*, 16588–16592; *Angew. Chem.* **2017**, *129*, 16815–16819.

[16] a) K. Stefkova, M. J. Heard, A. Dasgupta, R. L. Melen, *Chem. Commun.* **2021**, *57*, 6736–6739; b) Y. Zhao, D. Mandal, J. Guo, Y. Wu, D. W. Stephan, *Chem. Commun.* **2021**, *57*, 7758–7761; c) A. Dasgupta, R. Babaahmadi, B. Slater, B. F. Yates, A. Ariafard, R. L. Melen, *Chem* **2020**, *6*, 2364–2381; d) A. Dasgupta, K. Stefkova, R. Babaahmadi, L. Gierlichs, A. Ariafard, R. L. Melen, *Angew. Chem. Int. Ed.* **2020**, *59*, 15492–15496; *Angew. Chem.* **2020**, *132*, 15621–15626; e) J. P. Mancinelli, S. M. Wilkerson-Hill, *ACS Catal.* **2020**, *10*, 11171–11176; f) Q. Zhang, X.-F. Zhang, M. Li, C. Li, J.-Q. Liu, Y.-Y. Jiang, X. Ji, L. Liu, Y.-C. Wu, *J. Org. Chem.* **2019**, *84*, 14508–14519; g) H. H. San, C.-Y. Wang, H.-P. Zeng, S.-T. Fu, M. Jiang, X.-Y. Tang, *J. Org. Chem.* **2019**, *84*, 4478–4485; h) H. H. San, S.-J. Wang, M. Jiang, X.-Y. Tang, *Org. Lett.* **2018**, *20*, 4672–4676; i) Z. Yu, Y. Li, J. Shi, B. Ma, L. Liu, J. Zhang, *Angew. Chem. Int. Ed.* **2016**, *55*, 14807–14811; *Angew. Chem.* **2016**, *128*, 15027–15031.

[17] G. Xu, C. Zhu, W. Gu, J. Li, J. Sun, *Angew. Chem. Int. Ed.* **2015**, *54*, 883–887; *Angew. Chem.* **2015**, *127*, 897–901.

[18] For selected reviews see: a) O. I. Afanasyev, E. Kuchuk, D. L. Usanov, D. Chusov, *Chem. Rev.* **2019**, *119*, 11857–11911; b) A. Ruffoni, F. Juliá, T. D. Svejstrup, A. J. McMillan, J. J. Douglas, D. Leonori, *Nat. Chem.* **2019**, *11*, 426–433.

[19] For selected reviews see: a) B. Han, X.-H. He, Y.-Q. Liu, G. He, C. Peng, J.-L. Li, *Chem. Soc. Rev.* **2021**, *50*, 1522–1586; b) V. Kumar, K. Kaur, G. K. Gupta, A. K. Sharma, *Eur. J. Med. Chem.* **2013**, *69*, 735–753; also see: c) A. Ansari, A. Ali, M. Asif, *New J. Chem.* **2017**, *41*, 16–41.

[20] J. H. Hansen, B. T. Parr, P. Pelphrey, Q. Jin, J. Autschbach, H. M. L. Davies, *Angew. Chem. Int. Ed.* **2011**, *50*, 2544–2548; *Angew. Chem.* **2011**, *123*, 2592–2596.

[21] B. Wang, H. Yi, H. Zhang, T. Sun, Y. Zhang, J. Wang, *J. Org. Chem.* **2018**, *83*, 1026–1032.

[22] B. N. Thomas, P. J. Moon, S. Yin, A. Brown, R. J. Lundgren, *Chem. Sci.* **2018**, *9*, 238–244.

[23] D. Zhang, G. Xu, D. Ding, C. Zhu, J. Li, J. Sun, *Angew. Chem. Int. Ed.* **2014**, *53*, 11070–11074; *Angew. Chem.* **2014**, *126*, 11250–11254.

[24] X. Zhao, Y. Zhang, J. Wang, *Chem. Commun.* **2012**, *48*, 10162–10173.

[25] J. R. Manning, H. M. L. Davies, *Org. Synth.* **2007**, *84*, 334–346.

[26] D. Drikermann, V. Kerndl, H. Görls, I. Vilotijevic, *Synlett* **2020**, *31*, 1158–1162.